Journal of Materials Chemistry A

Accepted Manuscript

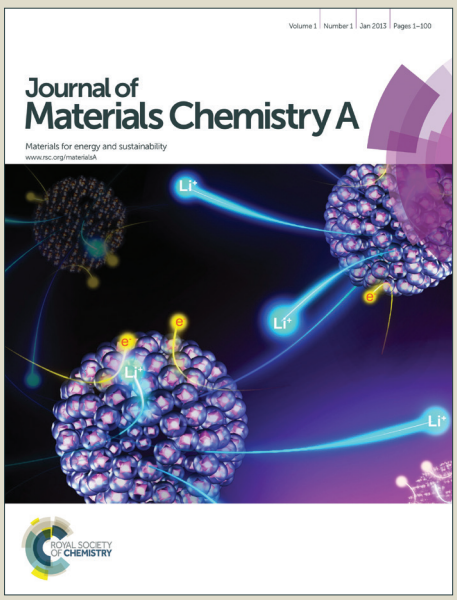

ROYAL SOCIETY OF CHEMISTRY

www.rsc.org/materialsA

Journal Name

RSCPublishing

ARTICLE

The epitaxial growth of lead-phthalocyanine on copper halogen compounds as the origin of templating effects

Cite this: DOI: 10.1039/x0xx00000x

Received 00th January 2012,
Accepted 00th January 2012

DOI: 10.1039/x0xx00000x

www.rsc.org/

Tae-Min Kim,[a] Hyo Jung Kim,[b] Hyun-Sub Shim,[a] Min-Soo Choi,[a] Ji Whan Kim,[a] and Jang-Joo Kim[a,*]

Templating effects on the growth of lead-phthalocyanine (PbPc) and the performance of organic photovoltaic cells (OPVs) have been investigated by using three copper halogen compounds (CuCl, CuBr, CuI) possessing different lattice parameters as the templating layers. The crystallinity of the PbPc films was the highest on CuI followed by CuBr and CuCl, resulting in the broadening of Q-band absorption in the same order. The templating effects were able to be described by heteroepitaxial growth of organic molecules on the templating layers and the dimensionless potential calculated using a lattice model for the overlayer-substrate systems showed good correlation between the degree of epitaxy and the crystallinity of PbPc overlayers. Furthermore, the performance of OPVs was consistent with the prediction from the calculation results and the observation from the optical and structural analyses.

Introduction

The control of the crystal structure and the orientation of the molecules is an important research topic in organic electronics such as organic photovoltaics (OPVs) and organic thin film transistors (OTFTs) because the optical and electrical properties of the films strongly depend on them. One of the methods to control the crystal structure of molecules is to use a templating layer. The organic templating layers such as 3,4,9,10-perylenetetracarboxylic dianhydride (PTCDA), 2,5-bis(4-biphenylyl)-bithiophene (BP2T), oxovanadium phthalocyanine (VOPc), sexithiophene (6T), para-sexiphenylene (*p*-6P), diindenoperylene (DIP) and pentacene have been used to control the crystal structure and/or the crystallinity of organic donor materials such as metal phthalocyanines.[1-9] Recently, CuI has been introduced as an effective templating material to control the crystal structure or the molecular orientation of copper phthalocyanine, zinc phthalocyanine and lead phthalocyanine (PbPc) molecules.[10-19] The OPVs showed nearly 2 times enhancement in a power conversion efficiency (PCE) by inserting the CuI templating layer. However, there are few reports on the mechanism of the templating effect of the CuI layer and it is not clearly understood yet.

In this work, we report that the templating effects originate from the epitaxial growth of organic molecules. CuCl, CuBr and CuI possessing different lattice spacings were selected as the templating layers. In addition, the PbPc was used as the organic donor material to analyse the templating effect because the increase of the crystallinity of PbPc film is easily noticed from change in absorption peaks at the wavelength of 740 nm and 900 nm which are related to the amorphous or the monoclinic phases and the triclinic phases.[14,19,20] The dimensionless potentials between the copper halogen compound substrates and the PbPc overlayer calculated using a lattice model showed that the degree of epitaxy increases in the sequence of CuCl, CuBr and CuI, consistent with the experimental results of the crystallinity and absorption of the PbPc films on the templating layers and the resulting device performance.

Experimentals

The control device had the following planar heterojunction structure: indium tin oxide (ITO) (150 nm)/ PbPc (20 nm)/ C_{60} (40 nm)/ BCP (8 nm)/ Al (100 nm). The ITO-coated glass substrate was successively cleaned with acetone and isopropyl alcohol. The substrate was exposed to UV-O_3 for 10 min before use. All the organic layers were deposited using thermal evaporation at the base pressure of ca. 10^{-7} torr with a rate of 1 Å/s without breaking the vacuum. CuCl, CuBr and CuI layers were also thermally deposited onto the substrate with a rate of 0.2 Å/s. The devices had active areas of 2×2 mm^2. A patterned insulator on the ITO and the top cathode deposited through a shadow mask defined the cell area. After fabrication, the devices were encapsulated using an epoxy resin with glass cans in an N_2 environment. More than 8 cells for each device structure were fabricated and the mean values of the photovoltaic performances and standard deviations were obtained. The photovoltaic properties of the devices were measured with an AM 1.5G 100 $mWcm^{-2}$ solar simulator (300 W Oriel 69911A) light source and a source measurement unit (Keithley 237). The measurement set up was calibrated with a National Renewable Energy Laboratory-certified reference Si-solar cell covered with a KG-5 filter before every measurement. The UV–vis absorption spectra of films were recorded with a VARIAN Cary 5000 UV–vis spectrophotometer. The

crystalline structures were investigated by synchrotron x-ray diffraction measurements at 5A x-ray scattering beamline for materials science of Pohang Light Source II (PLS-II). The x-ray wavelength was 1.071 Å (11.58 KeV). The films were deposited on ITO substrates. Atomic force microscope (AFM) topographic images of the films were taken using a PSIA XE-100 scanning probe microscope in the non-contact mode.

Results and Discussion

The templating effect of the copper halogen compounds on the absorption of the PbPc films is shown in Fig. 1. The 20 nm-thick PbPc film was deposited on 3 nm-thick CuCl, CuBr and CuI coated ITO substrates. The intensity of the absorption peak at the wavelength of 740 nm in the Q-band absorption of PbPc is gradually reduced in the order of CuCl, CuBr and CuI and the peak at 900 nm is newly developed in the same order resulting in the two times enhancement by inserting the CuI layer. The broadened Q-band absorption of the PbPc film can be assigned as the increase of the monoclinic phase in the film.[14] The grazing incident angle x-ray diffraction (GIXD) was performed with the incident angle of 0.2° to investigate the crystalline property of the PbPc films and the GIXD patterns of the samples are depicted in Fig. 2(a). The pristine 20 nm-thick PbPc film on ITO without the templating layers shows the diffraction peaks at Q = 8.89 nm^{-1} and Q = 11.72 nm^{-1} which are assigned as the (320) plane of the monoclinic PbPc phase and $(1\bar{3}0)$ plane of the triclinic phase, respectively.[14,20] The diffraction peak of the $(1\bar{2}1)$ plane of the triclinic phase is shown at Q = 9.15 nm^{-1}.[20] The intensity of the diffraction peak of the (320) plane of the monoclinic PbPc phase gradually increased in the order of CuCl, CuBr and CuI, which is the same tendency as the broadening of the Q-band absorption peak.

The diffraction patterns of the same samples after the deposition of a 40 nm-thick of C_{60} layer on top of the PbPc layers are shown in Fig. 2(b). The diffraction peaks at Q = 7.69 nm^{-1}, Q = 12.64 nm^{-1} and Q = 14.87 nm^{-1} are assigned as the (111) plane, (220) plane and (311) plane of the face centered cubic (FCC) phase of C_{60}.[18] The diffraction peaks of (320) plane of the monoclinic PbPc phase and $(1\bar{2}1)$ plane of the triclinic PbPc phase disappeared after the deposition of the C_{60} layer, indicating that the crystal structure is demolished by the

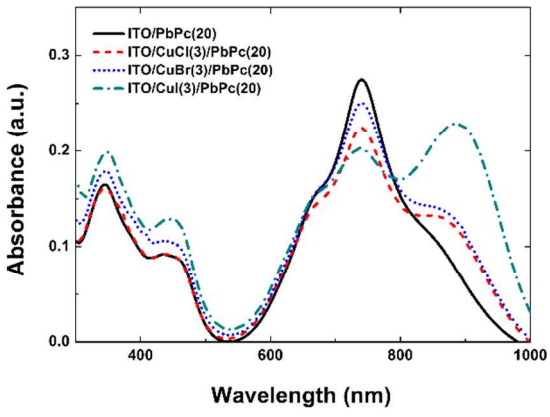

Figure 1. The absorption spectra of pristine 20 nm-thick PbPc film grown on ITO (black line) and films grown on 3 nm-thick CuCl (red dashed line), CuBr (blue dot line) and CuI (green dashed dot line) deposited on the ITO substrates, respectively.

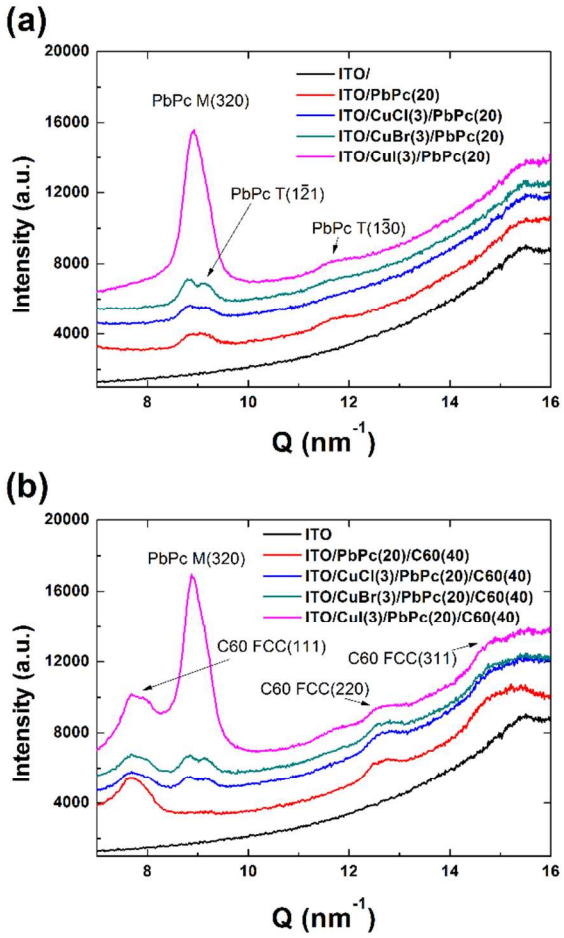

Figure 12. (a) The X-ray diffraction patterns of ITO (black), PbPc (20 nm) (red), CuCl (3 nm)/PbPc (20 nm) (blue), CuBr (3 nm)/PbPc (20 nm) (green) and CuI (3 nm)/PbPc (20 nm) (pink) deposited on the ITO pre-coated glass. (b) The X-ray diffraction patterns of the films after the deposition of C_{60} layer on top of the PbPc layer.

deposition of the C_{60} molecules due to the interaction with C_{60} at the interface or the diffusion of C_{60} molecules into the organic layer. It can take place because large portion of the PbPc crystalline is located near the surface, exhibiting the thickness dependent phase transition.[20] However, the diffraction peaks of PbPc grown on the copper halogen compounds are retained after the deposition of C_{60} layer, indicating that the crystalline PbPc in the film grown on the copper halogen compounds is less affected by the deposition of C_{60} layer because it locates near the interface of the copper halogen compounds/PbPc or distributed in the whole layer.

The templating effect was analysed based on the concept of heteroepitaxy where the molecule-substrate bonding due to electrostatic interactions between the molecules and the anion in the ionic compounds is considered as the driving force to control the crystal structure and the molecular orientation of the organic molecules.[22-24] The dimensionless potential V/V_0 has been calculated by a simple analytic method to evaluate the heteroepitaxial system by considering the geometrical lattice mismatch.[25] This approach can analyse the phase coherence between an overlayer and substrate unit cells and describe their potential energy as simple plane waves which is modelled by cosine functions. The value of V/V_0 is determined by the degree of epitaxy between overlayer and substrate in the range $-0.5 <$

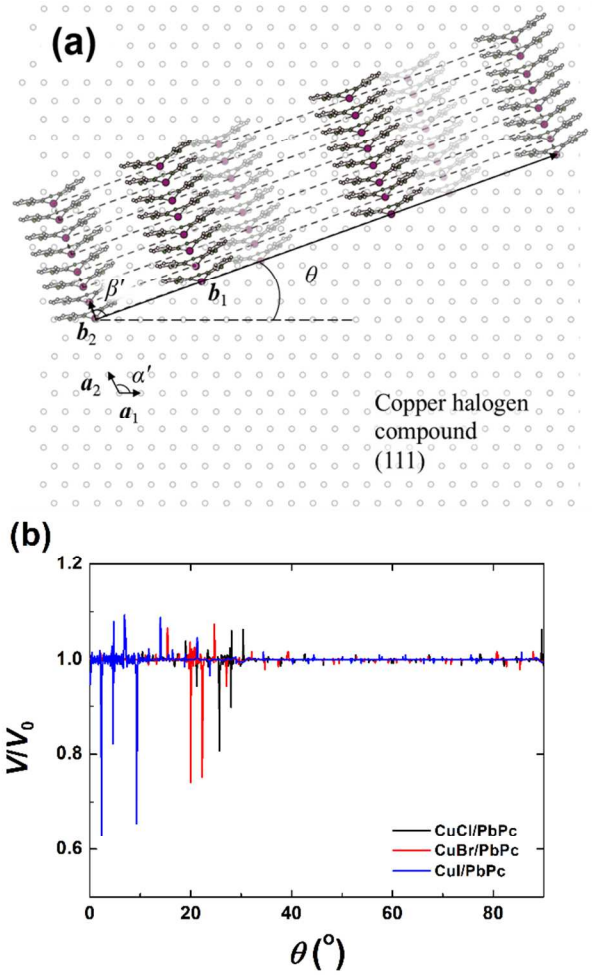

Figure 2. (a) Schematic representation of PbPc monoclinic (320) overlayers on copper halogen compounds. The parameters a_1, a_2 and α' of the substrates and b_1, b_2 and β' of the PbPc layer were calculated from the lattice parameters of the respective unit cells. The azimuthal angle θ represents the angle between the vector a_1 and b_1. (b) Calculated V/V_0 against azimuthal angle θ of PbPc overlayer on CuCl (black line), CuBr (red line) and CuI (blue line), respectively.

$V/V_0 < 1$ where $V/V_0 = 1$ for incommensurism, $V/V_0 = 0.5$ for coincidence, $V/V_0 = 0$, $V/V_0 = -0.5$ for commensurism on a nonhexagonal and hexagonal substrates, respectively. First of all, we calculated the potential energy of the PbPc 55×55 overlayer on the series of copper halogen compounds with the lattice parameters ranging from 1 to 14 Å with 0.001 Å of grid. The copper halogen compounds have the zinc blende (111) structure on ITO substrates as shown in Fig. S1 and PbPc molecules are assumed to be grown with the monoclinic (320) structure dominantly on the copper halogen compounds.[12] The lattice parameters of the PbPc monoclinic phase and the copper halogen compounds used for the calculation are summarized in Table 1, which were taken from literature.[14,20,26-31] The schematic representation of the overlayer of PbPc monoclinic (320) and zinc blende (111) ionic compounds substrate are displayed and the seven parameters $\boldsymbol{a}_1$, $\boldsymbol{a}_2$, α' and $\boldsymbol{b}_1$, $\boldsymbol{b}_2$, β' for representing the unit cells and the azimuthal angle θ between the overlayer and the substrate unit cells used in the calculations are defined in Fig. 3(a). The dependences of the potential V/V_0 on azimuthal angle θ of PbPc 55×55 overlayer

Table 1. The lattice parameters of PbPc monoclinic and copper halogen compounds with zinc blende structure.

	a [Å]	b [Å]	c [Å]	$\alpha=\beta=\gamma$ [°]
PbPc	25.48	25.48	3.73	90
CuCl	5.424	5.424	5.424	90
CuBr	5.695	5.695	5.695	90
CuI	6.054	6.054	6.054	90

and CuCl, CuBr and CuI substrates used in our works are presented in Fig. 3(b). The calculation results predict the degree of epitaxy at specific angles. The minima of potential V/V_0 when using CuCl and CuBr show values of 0.81, 0.74, respectively. CuI showed the smallest potential V/V_0 value of 0.63 at θ of 2.3° among them, indicating that the PbPc monoclinic phase with the (320) orientation forms the coincidence epitaxy most favourably using CuI as the templating layer. The analysis predicts that the larger monoclinic crystals with better crystallinity are formed using the CuI templating layer followed by CuBr and CuCl, which are in good agreement with the experimental results. The consistency between the experimental results and the theoretical analysis suggests that the templating effects originate from the heteroepitaxial growth of the PbPc films on the copper halogen compounds. Furthermore, the crystal structure of the organic thin film is closely related with the lattice parameters of the ionic compounds. In other words, the organic thin film is grown toward minimizing the strain energy between the molecule-substrate lattice mismatch. Growth of organic molecules on ionic compounds such as KBr, KCl and NaCl was previously explained by a heteroepitaxy.[25,32,33]
The AFM images in Fig. 4 illustrate the variation of the surface morphology of the 5 nm-thick PbPc films on the different copper halogen compounds substrates. The initial growth of the several monolayer of PbPc molecules shows the Stranski-Krastanov (SK) mode on the CuI substrate and the Volmer-Weber (VW) mode on pristine ITO substrate due to the increase of the lattice mismatch.[34] The surface coverage is the largest on

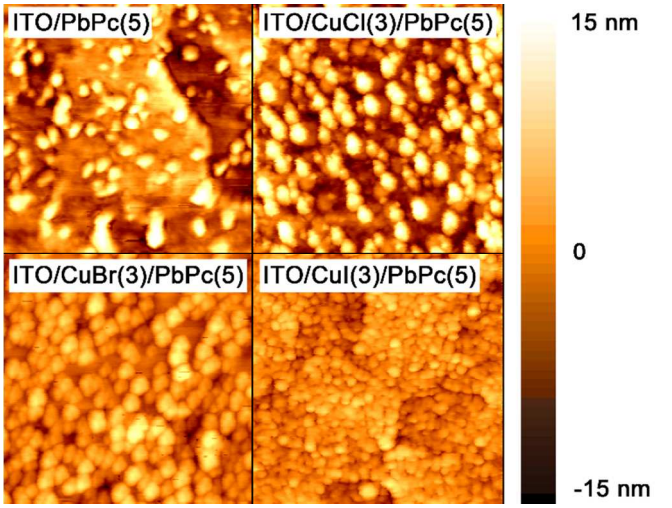

Figure 3. AFM images of the 5 nm-thick PbPc film grown on the ITO and 3 nm-thick CuCl, CuBr and CuI coated ITO substrate are displayed, respectively. The images are 1×1 μm^2

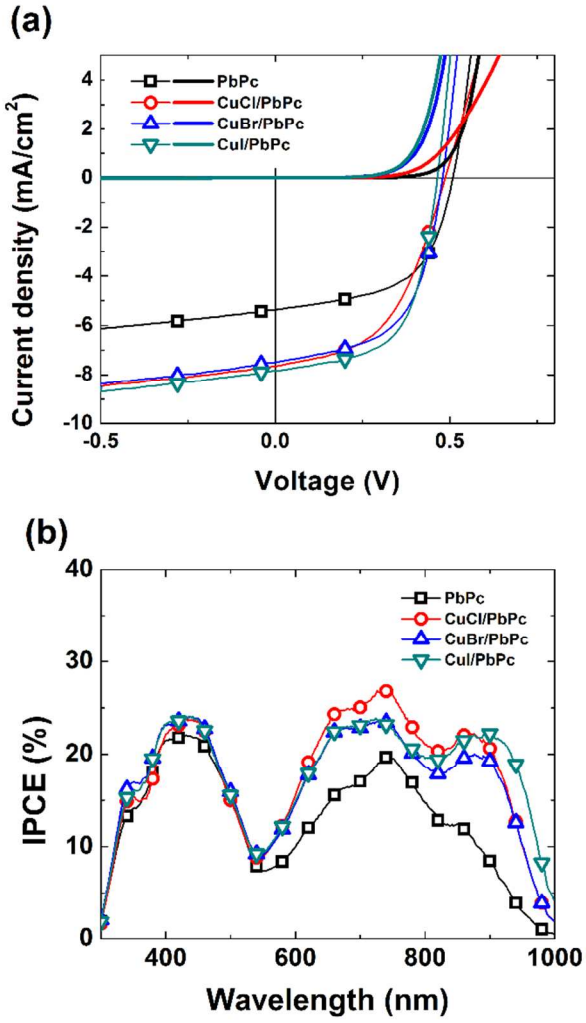

Figure 4. (a) The *J-V* characteristics of the OPVs with the copper halogen compounds. The control device (black square) is comprised of ITO/PbPc (20 nm)/C_{60} (40 nm)/BCP (8 nm)/Al. The devices with a 3 nm-thick CuCl (red circle) layer, 3 nm-thick CuBr (blue triangle) and 3 nm-thick CuI (green triangle) inserted between the ITO and PbPc layers in the control device are also shown. (b) The IPCE spectra of the PbPc based control device (black square) and devices with CuCl (red circle), CuBr (blue triangle) and CuI (green triangle) are displayed.

the CuI substrate and larger island of the PbPc with small coverage are formed on the pristine ITO substrate. The coverage of the PbPc films becomes larger with increase of the thickness of PbPc films.

The templating effects are manifested in the performance of the OPVs. The current density-voltage (*J-V*) characteristics of the devices formed on different templating layers are represented in Fig. 5(a). The photovoltaic parameters, the parallel resistance (R_P) and the series resistance (R_S) extracted from the dark *J-V* curves with the equivalent Shockley diode equation are summarized in Table 2. The control device showed the PCE of 1.53% with the short-circuit current density (J_{SC}) of 5.26 mAcm^{-2}, the open-circuit voltage (V_{OC}) of 0.52 V and the fill factor (*FF*) of 0.57. Insertion of the CuCl, CuBr and CuI templating layers enhanced J_{SC} to 7.67, 7.60, 7.89 mAcm^{-2}, thereby, the PCE to 1.82, 1.97, 2.10%, respectively. The lower *FF* of the device with CuCl is reflected in higher R_S of 13.84 Ωcm^2, which might be related to its deep valence band energy level (CuCl; 6.9 eV, CuBr; 5.6 eV, CuI; 5.0 eV) working as a potential barrier for hole-transport at the interface between ITO and active layer.[26] The increase of J_{SC} originates from the enhancement of incident photon-to-current efficiency (IPCE) in the part of PbPc molecules (Fig. 5(b)). In our previous work, the exciton diffusion length (L_D) increased with enhancement of crystallinity by insertion of the templating layer.[11] The GIXD results in Fig. 2(b) indicate that the copper halogen compounds prevent the PbPc film from losing the crystallinity after the deposition of C_{60} and it is the origin of higher L_D and IPCE of the devices with the copper halogen compounds. In addition, decrease of V_{OC} from 0.52 V to 0.47, 0.47, 0.45 V can be explained by the reduced band gap of the PbPc film due to the intermolecular interaction of molecules, manifested in the red-shifted absorption spectra of PbPc films and IPCE spectra of the devices with the copper halogen compounds. Since V_{OC} of OPVs is related with the energy level difference between the lowest unoccupied molecular orbital (LUMO) level of acceptor and the highest occupied molecular orbital (HOMO) level of donor material, the change in V_{OC} can be explained by the shift of energy level of PbPc film.

Conclusions

We have investigated the templating effect of copper halogen compounds on PbPc films using the theory of heteroepitaxy. Simple lattice modelling predicted that the PbPc monoclinic phase with the (320) orientation forms the coincidence epitaxy most favourably using CuI as the templating layer minimizing the potential energy due to the least lattice mismatch between the organic crystal and templating layer followed by CuBr and CuCl. The change of phase and the enhancement in crystallinity of the PbPc film on the copper halogen compounds are consistent with our calculation; more pronounced formation of

Table 2. The summary of photovoltaic parameters and R_P, R_S extracted from dark *J-V* curves by using Shockley equation of the devices with copper halogen compounds.

	PCE [%]	J_{SC} [mAcm^{-2}]	V_{OC} [V]	FF	R_P [×10^6 Ωcm^2]	R_S [Ωcm^2]
PbPc	1.53±0.013	5.26±0.086	0.52±0.016	0.57±0.013	5.07	3.07
CuCl/PbPc	1.82±0.056	7.67±0.103	0.47±0.016	0.51±0.012	0.11	13.84
CuBr/PbPc	1.97±0.101	7.60±0.093	0.47±0.008	0.55±0.036	0.15	3.33
CuI/PbPc	2.10±0.056	7.89±0.064	0.45±0.011	0.59±0.010	0.12	4.59

the PbPc monoclinic phase with the (320) orientation and enhanced crystallinity in the sequence of CuI>CuBr>CuCl. In addition, the initial growth modes of the PbPc films are influenced by the degree of the lattice mismatch between the organic crystal and templating layer. Large mismatch (PbPc on ITO) resulted in the island (VW) growth mode with low surface coverage but small mismatch (PbPc on CuI) resulted in the SK growth mode with much better surface coverage. Apparently the different growth modes on different templates influence the performance of the PbPc based OPV; the templating layer with less lattice mismatch resulted in higher PCEs in the sequence of CuI>CuBr>CuCl>none on ITO. We believe that the application of the concept of heteroepitaxy is not limited to our specific system but can be a general phenomenon in organic/organic and organic/inorganic multilayer systems and the degree of the heteroepitaxy depends on the interaction energy between the templating layer and the overlayer. This heteroepitaxy must have the important application not only in OPVs and OTFTs but also in every area where organic crystalline structure plays importance roles.

Acknowledgements

This work was supported by the New & Renewable Energy Technology Development Program of the Korea Institute of Energy Technology Evaluation and Planning (KETEP) grant funded by the Korea government Ministry of Trade, Industry and Energy (no. 20113020010070).

Notes and references

[a] Department of Materials Science and Engineering and the Center for Organic Light Emitting Diode, Seoul National University, Seoul 151-744, South Korea

[b] Department of Organic Material Science and Engineering, College of Engineering, Pusan National University, Busan 609-735, South Korea

Electronic Supplementary Information (ESI) available: [details of any supplementary information available should be included here]. See DOI: 10.1039/b000000x/

1 P. Sullivan, T. S. Jones, A. J. Ferguson and S. Heutz, *Appl. Phys. Lett.*, 2007, **91**, 233114.
2 J. Yang and D. Yan, *Chem. Soc. Rev.*, 2009, **38**, 2634.
3 B. Yu, L. Huang, H. Wang and D. Yan, *Adv. Mater.*, 2010, **22**, 1017.
4 T. Sakurai, T. Ohashi, H. Kitazume, M. Kubota, T. Suemasu and K. Akimoto, *Org. Electron.*, 2011, **12**, 966.
5 W. Zhao, J. P. Mudrick, Y. Zheng, W. T. Hammond, Y. Yang and J. Xue, *Org. Electron.*, 2012, **13**, 129.
6 S. S. Roy, D. J. Bindl and M. S. Arnold, *J. Phys. Chem. Lett.*, 2012, **3**, 873.
7 K. Xiao, W. Deng, J. K. Keum, M. Yoon, I. V. Vlassiouk, K. W. Clark, A.-P. Li, I. I. Kravchenko, G. Gu, E. A. Payzant, B. G. Sumpter, S. C. Smith, J. F. Browning and D. B. Geohegan, *J. Am. Chem. Soc.*, 2013, **135**, 3680.
8 Y. Zhou, T. Taima, T. Kuwabara and K. Takahashi, *Adv. Mater.*, 2013, **25**, 6069.
9 S. Kawata, Y.-J. Pu, C. Ohashi, K.-I. Nakayama, Z. Hong and J. Kido, *J. Mater. Chem. C*, 2014, **2**, 501
10 C. H. Cheng, J. Wang, G. T. Du, S. H. Shi, Z. J. Du, Z. Q. Fan, J. M. Bian and M. S. Wang, *Appl. Phys. Lett.*, 2010, **97**, 083305.
11 H.-S. Shim, H. J. Kim, J. W. Kim, S.-Y. Kim, W.-I. Jeong, T.-M. Kim and J.-J. Kim, *J. Mater. Chem.*, 2012, **22**, 9077.
12 T.-M. Kim, J. W. Kim, H.-S. Shim and J.-J. Kim, *Appl. Phys. Lett.*, 2012, **101**, 113301.
13 B. P. Rand, D. Cheyns, K. Vasseur, N. C. Giebink, S. Mothy, Y. Yi, V. Coropceanu, D. Beljonne, J. Cornil, J.-L. Brédas and J. Genoe, *Adv. Funct. Mater.* 2012, **22**, 2987.
14 H. J. Kim, H.-S. Shim, J. W. Kim, H. H. Lee and J.-J. Kim, *Appl. Phys. Lett.* 2012, **100**, 263303.
15 Y. Zhou, T. Taima, T. Miyadera, T. Yamanari, M. Kitamura, K. Nakatsu and Y. Yoshida, *Nano Lett.*, 2012, **12**, 4146.
16 Y. Zhou, T. Taima, T. Miyadera, T. Yamanari, M. Kitamura, K. Nakatsu and Y. Yoshida, *Appl. Phys. Lett.*, 2012, **100**, 233302.
17 J. W. Kim, H. J. Kim, T.-M. Kim, T. G. Kim, J.-H. Lee, J. W. Kim and J.-J. Kim, *Curr. Appl. Phys.*, 2013, **13**, 7.
18 J. C. Bernede, L. Cattin, M. Makha, V. Jeux, P. Leriche, J. Roncali, V. Froger, M. Morsli and M. Addou, *Sol. Energy Mater. Sol. Cells*, 2013, **110**, 107.
19 K. Vasseur, K. Broch, A. L. Ayzner, B. P. Rand, D. Cheyns, C. Frank, F. Schreiber, M. F. Toney, L. Froyen and P. Heremans, *ACS Appl. Mater. Interfaces*, 2013, **5**, 8505.
20 K. Vasseur, B. P. Rand, D. Cheyns, L. Froyen and P. Heremans, *Chem. Mater.*, 2011, **23**, 886.
21 W. Zhao, W.-L. Zhou, L.-Q. Chen, Y.-Z. Huang, Z.-B. Zhang, K. K. Fung, Z.-X. Zhao, *J. Solid State Chem.*, 1994, **112**, 412.
22 A. Koma, Prog. *Crystal Growth and Charact.*, 1995, **30**, 129.
23 S. R. Forrest, *Chem. Rev.*, 997, **97**, 1793.
24 S. R. Forrest and P. E. Burrows, *Supramol. Sci.*, 1997, **4**, 127.
25 D. E. Hooks, T. Fritz and M. D. Ward, *Adv. Mater.*, 2001, **13**, 227.
26 S. Kono, T. Ishii, T. Sagawa and T. Kobayasi, *Phys. Rev. B*, 1973, **8**, 795.
27 S. Hull and D. A. Keen, *Phys. Rev. B*, 1994, **50**, 5868.
28 A. Miyamoto, K. Nichogi, A. Taomoto, T. Nambu and M. Murakami, *Thin Solid Films*, 1995, **256**, 644.
29 L. Ottaviano, L. Lozzi, A.R. Phani, A. Ciattoni, S. Santucci and S. Di Nardo, *Appl. Surf. Sci.*, 1998, **136**, 81.
30 K.Mizoguchi, K. Mizui, D. G. Kim and M. Nakayama, *Jpn. J. Appl. Phys.*, 2002, **41**, 6421.
31 S. Tabuchi, H. Tabata and T. Kawai, *Surf. Sci.*, 2004, **571**, 117.
32 D.-M. Smilgies and E. J. Kintzel, Jr., *Phys. Rev. B*, 2009, **79**, 235413.
33 E. Lorenz, C. Keil and D. Schlettwein, *J. Porphyrins Phthalocyanines*, 2012, **16**, 977.
34 I. Daruka, A.-L. Barabási, *Phys. Rev. Lett.*, 1997, **79**, 3708.